Trajectory Study of Photodissociation Dynamics in the NaI(H_2O) Cluster System

Gilles H. Peslherbe,[†,‡] Branka M. Ladanyi,*[,‡] and James T. Hynes*[,†,§]

Department of Chemistry and Biochemistry, University of Colorado, Boulder, Colorado 80309-0215, Department of Chemistry, Colorado State University, Fort Collins, Colorado 80523, and Laboratoire de Photophysique Moléculaire du CNRS, Université Paris-Sud, 91405 Orsay, France

Received: November 18, 1997; In Final Form: January 30, 1998

The photodissociation dynamics of the NaI(H_2O) dimer is studied theoretically. The dynamics are simulated via the "molecular dynamics with quantum transitions" trajectory method of Tully and co-workers in order to describe nonadiabatic transitions between the excited and ground electronic states. In the calculations, the electronic structure of NaI is determined at every point along trajectories by semiempirical valence-bond theory, while the water is described by classical potentials. It is found that the clustered water enhances the probability of an excited-to-ground-state nonadiabatic transition compared to the isolated NaI case. In addition, the clear oscillatory dynamics for the bound excited state motion for isolated NaI is considerably muted by the presence of the water. Other characteristic features of the process include a considerable transfer of rotational kinetic energy to the water molecule and a rapid "evaporation" of that molecule. These latter characteristic features are shown to arise from a reversed polarity of the Franck−Condon excited state NaI compared with the ground state polarity $Na^{+\delta}I^{-\delta}$.

I. Introduction

The NaI system has become the prototype system for the study of photodissociation dynamics involving curve crossing of covalent and ionic states.[1−9] In particular, pioneering experiments by Zewail and co-workers[1−4] have probed the real-time dynamics in the excited state both of the bound motion and of the predissociation. Briefly, photoexcitation of the ground-state NaI to the first excited state results in bound oscillatory motion in the excited state potential, modulated by predissociation to the ground state. The latter arises from the crossing of the diabatic covalent and ionic curves, which are electronically coupled. Equivalently, there are nonadiabatic transitions from the excited adiabatic state to the ground adiabatic state due to the nuclear motion, to produce dissociated Na and I atoms.[10,11] The NaI photodissociation dynamics has also been the focus of a number of theoretical studies, exploiting a variety of methodologies.[8,9]

Our own interest in NaI has centered on the photodissociation dynamics for this system in solution,[12] and this has led to the present, first installment of the dynamics in clusters. Briefly, our earlier work[12] suggested that activated electron transfer (ET) might occur in small clusters, which are sufficiently large to involve significant solvation and "solvent" reorganization but sufficiently small so that associated barriers would be small enough to allow activated ET to compete with radiative decay to an environmentally stabilized ground ionic state. Although this has provided one motivation to begin the cluster studies, such studies are of independent fundamental interest and are the subject of current experiments at Orsay and Saclay.[13] A number of earlier theoretical studies have focused on the dynamics of chemical reactions in clusters.[14]

In this paper, we examine photodissociation dynamics of the NaI·H_2O system, focusing particularly on mechanistic aspects and the differences compared to the isolated NaI case. In separate contributions we will describe the structures of NaI-$(H_2O)_n$ clusters[15] and dynamics in larger cluster systems.[16]

The outline of the present paper is as follows. The potentials and dynamics of the isolated NaI system, briefly described in section II, are not treated in all generality or at the highest possible level of accuracy but rather at a sufficiently realistic level to address the more complex NaI·H_2O system. Section III begins the discussion of the latter, focusing on charge distributions, potentials, and structures for NaI·H_2O. The photodissociation dynamics of NaI·H_2O is presented in section IV, while section V concludes.

II. Isolated NaI Photodissociation

In this section, we describe the potentials employed for and the excited state dynamics of the bare NaI system, in preparation for the NaI·H_2O system described in the remaining sections.

A. Potentials. For the ground and excited adiabatic states of NaI, we use the potentials developed in previous work and reported in an earlier publication,[12] to which the reader is referred for details. Briefly, we employ a semiempirical valence-bond (VB) theory, where the ground and excited adiabatic states of NaI are taken to be linear combinations of diabatic, constant-charge character, and ionic Na^+I^- and covalent NaI VB states, and the Hamiltonian matrix elements (or other properties) of these VB states are calculated with semiempirical quantum chemistry. In our semiempirical model, only two electrons are treated explicitly for NaI, while the contribution due to the remaining electrons is embedded in a core−core potential. Further, all electron integrals are evaluated under the point-charge, Pariser and Mulliken approximations,[17] resulting in analytical expressions for all diabatic matrix elements. The adiabatic energies are then just obtained by diagonalizing the Hamiltonian matrix in the VB state basis. In contrast to our earlier work,[12] we adjusted the core−core potential parameters *separately* for both VB states in order to

[†] University of Colorado.
[‡] Colorado State University.
[§] Orsay. Permanent address: University of Colorado.

S1089-5639(98)00253-9 CCC: $15.00
Published on Web 04/08/1998

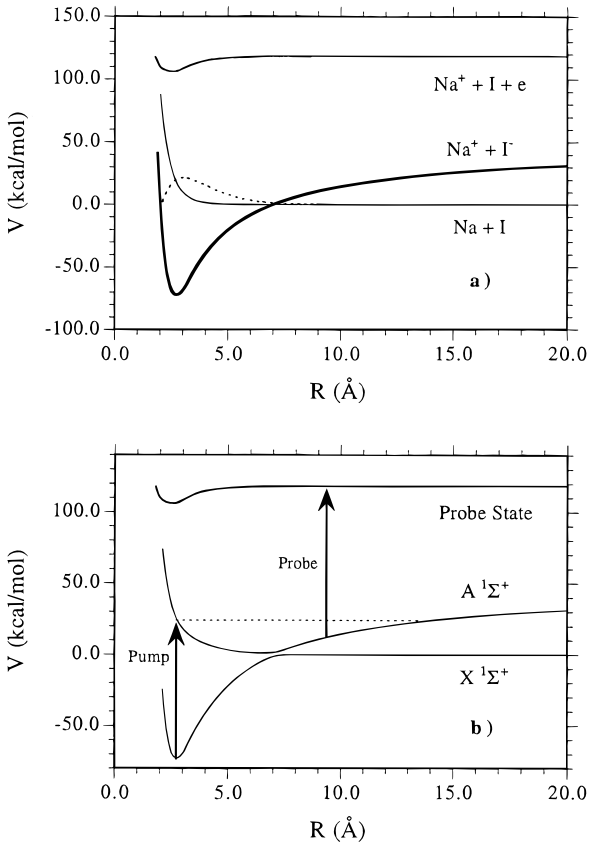

Figure 1. NaI potential energy curves: (a) diabatic ionic, covalent, and probe state energy curves, where the dashed line represents the electronic coupling between the ionic and covalent states; (b) resulting adiabatic energy curves and experimental pump−probe setup.

better reproduce the experimental Franck−Condon (FC) excess energy in the excited state. With the latter parametrization of the core−core potentials, the gas-phase NaI Franck−Condon excitation wavelength is 296 nm, which lies at the lower end of the experimental range of excitation wavelengths.[2] For instance, the calculated FC excess energy in the excited adiabatic state is 24 kcal/mol, while its experimental counterpart is 22.5 and 18.5 kcal/mol for typical experiments carried out at 300 and 312 nm, respectively.[2b] The NaI potentials, displayed in Figure 1, are in overall reasonable agreement not only with results from experiments but also with results from high-level ab initio calculations.[16,18]

We postpone presentation of the charge distributions of the ground and excited NaI states until section III.A, where they are more conveniently discussed in connection with the interaction of NaI with the water molecule.

There is another potential to be generated, motivated by the Orsay/Saclay detection scheme of Jouvet et al.[6] for NaI, in which excitation is made to a probe state that asymptotically correlates to $Na^+ + I + e$, and this is dominated (roughly) by transitions out of the excited adiabatic state corresponding to the ionic branch. This probe state potential is also determined with our semiempirical quantum chemistry approach, and the core−core potential for this state was adjusted to yield a INa^+ binding energy of ∼0.5 eV, as was done in previous work.[6,8a] The long-range part of the potential is essentially just a $-\alpha_I/(2R^4)$ term arising from the polarization of iodine due to the sodium ion, where α_I is the polarizability of iodine and R is the NaI internuclear separation. We use $\alpha_I = 5.35$ Å^3,[19] and the resulting potential is slightly less attractive[20] than that of Jouvet et al.[6] and much less attractive than that postulated by Engel et al.[8a] However, we found that the choice of the probe state potential has little impact on the resulting simulated photodissociation probe signals. Finally, note that the diabatic probe state is not included when solving for the first two adiabatic states of NaI, since it lies very high in energy and, thus, does not mix with the ionic Na^+I^- and covalent NaI states.

B. MD Simulations and Curve-Crossing Dynamics. *(i) Simulation Method.* In this paper, we employ a "surface-hopping" trajectory method known as the "molecular dynamics with quantum transitions" (MDQT) method, developed by Tully and co-workers,[21] to follow the dynamics in the excited electronic state and the decay to the ground state. It should be immediately noted that, because the nuclear degrees of freedom are treated classically, the coherence of the nuclear wave function is not taken into account in our calculations, and Franck−Condon factors, which can be important in describing photon absorption and curve-crossing phenomena, are neglected. However, a detailed comparison with a full quantum mechanical treatment shows that classical mechanics indeed allows an adequate description of the NaI photodissociation dynamics,[8c] and thus, we follow this route, which should also be adequate for the NaI(H_2O) system, where the water is described by classical potentials as discussed in section III; further, this is the only presently feasible approach for our future studies of the photodissociation dynamics of larger NaI$(H_2O)_n$ clusters.

In the MDQT method, the classical particles (nuclei) are constrained to evolve on an individual adiabatic (electronic) potential energy surface, while the actual quantum system should evolve as a mixture of coupled quantum states. The essence of the mixed quantum/classical dynamics "surface-hopping" trajectory methods is to let the adiabatic states evolve into mixed quantum states and project them back into a new adiabatic basis: classical and quantal degrees of freedom are propagated simultaneously, and at each trajectory time step, the quantum subsystem time evolution dictates the choice of which adiabatic potential energy surface the dynamics will be propagated on in the following time step. Typically, a time-dependent wave function expanded in terms of the electronic adiabatic states is propagated together with the classical nuclear motion, and a key ingredient in the equations of motion for the quantum degrees of freedom is the nonadiabatic coupling vector between the electronic states.[22]

With the MDQT method, transitions can occur anywhere along trajectories, not just at localized avoided crossings. Further, quantum coherences between different state switches are maintained. At each trajectory time step, the probability of undergoing a transition is calculated from the time-dependent wave function expansion coefficients, and a stochastic "fewest switches" algorithm is used to decide whether a hop to another adiabatic state should occur or not. If a switch between states is performed, the energy difference between the states is distributed among the various classical degrees of freedom along the nonadiabatic coupling vector.[21] In the MDQT method, each trajectory is propagated completely coherently; that is, values of the coefficients of the time-dependent wave function are retained throughout the propagation so that memory of the coupling between quantum states is preserved at all times, which allows possible multiple crossings to be described properly along one trajectory. However, to account for quantum decoherence, one needs to propagate a swarm of trajectories for a given single classical initial condition. Each swarm trajectory follows its own path, since surface switches occur at different times along the trajectory, owing to different random number sequences in the stochastic process. The resulting spreading of trajectories

leads to a loss of phase coherence when summing the results over all trajectories.[23] Test calculations showed that a swarm of 100 trajectories was sufficient to obtain converged results for the NaI curve-crossing dynamics, and we shall use this swarm size thereafter.

In MDQT simulations, and more generally in simulations[24] where all or part of the system is described by quantum chemistry/mechanics and the remaining part is described with classical potentials, the "quantum" forces on the nuclei are customarily computed via the Hellmann−Feynman theorem,[25] which offers a convenient inexpensive route for calculating energy gradients for the quantum subsystem.[26] However, because the latter theorem only applies to true stationary state wave functions that satisfy the Schroedinger equation, Hellmann−Feynman forces can be grossly in error when using incomplete basis sets,[27] and in our two VB-state basis, they were. Thus, analytical expressions for the forces with the mixed semiempirical VB theory/classical potentials have been derived. The nuclear motion is propagated classically with the "velocity" version[28] of the Verlet algorithm,[29] and a step size of 0.2 fs, which ensures excellent energy conservation.

In contrast to earlier applications of the MDQT method,[21] where the propagation of the time-dependent wave function relied on a number of numerical approximations, the present mixed semiempirical VB/classical potential representation allows one to compute the elements of the nonadiabatic coupling vector analytically so that the propagation of the quantum degrees of freedom reduces to a two-point boundary-value problem, which is solved efficiently and accurately by a second-order finite-difference-equation numerical method.[30]

(ii) Initial Conditions and Detection Scheme. The initial condition for the isolated NaI photodissociation dynamics is obtained by promoting NaI at the ground ionic state potential minimum to the excited adiabatic state via a vertical transition (296 nm), hereby neglecting temperature effects, which may account for at most a few kcal/mol of additional excitation energy. The resulting excess FC energy is 24 kcal/mol. With this simple choice of initial conditions, the spreading of total energies for the photoexcited species due to the finite pump laser pulse is neglected. But we do not expect the latter to have dramatic effects on the main features and mechanism of the photodissociation dynamics of the isolated NaI or the NaI·H_2O cluster system discussed later. Meanwhile, the finite laser pulse width of the pump, as well as that of the probe, is taken into consideration in calculating the simulated probe signal, which is to be ultimately compared with results from cluster photodissociation experiments,[31] as discussed below.

Finally, we apply essentially the same detection scheme as the one reported by Jouvet et al.[6] For each time delay between excitation and detection, the species trapped in the first excited adiabatic state well, and only those for which the excited adiabatic state is predominantly ionic, undergo a vertical 263-nm (probe wavelength) excitation. Basically, if the total energy of the freshly excited species exceeds that of the probe state, the species are promoted to the asymptotically $Na^+ + I + e$ probe state. The outgoing electron is then ejected with an energy corresponding to the energy difference between the probe and the first excited state shifted by the ionizing probe photon energy, while the kinetic energy of the nuclei remains unaffected. As done previously,[6] the newly ionized species are considered dissociated if their internal kinetic energy exceeds the INa^+ binding energy. The resulting histogram distributions for detection of various probe species, such as Na^+, are convoluted with a Gaussian function, with variance of 250 fs,[6]

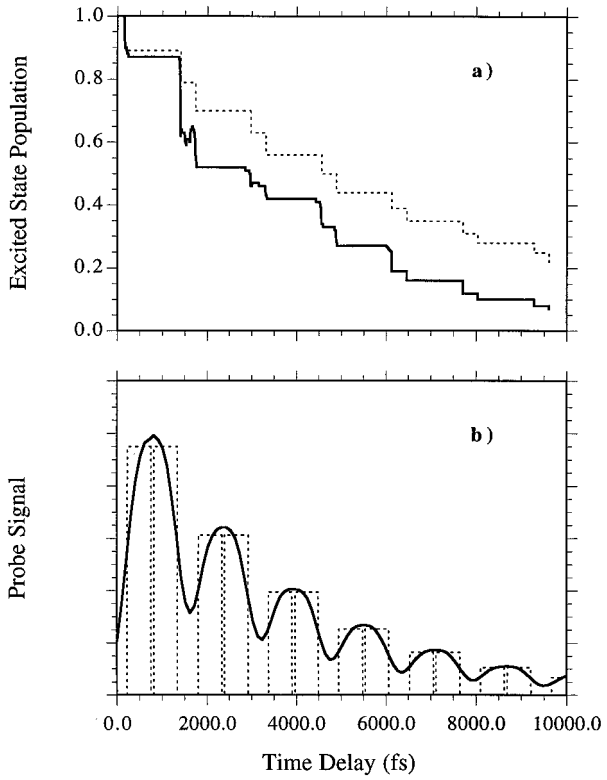

Figure 2. Isolated NaI photodissociation dynamics results: (a) excited adiabatic state time-dependent population calculated with the MDQT method (solid line) and the Landau−Zener model (dashed line); (b) Na^+ ion probe signal. The dashed line represents the histogram data collected from the MD simulation, while the solid line represents the simulated signal resulting from a convolution of the histogram results with a Gaussian pulse function. The probe signal first rises, since the probe state is only accessible from the outer, ionic branch of the excited adiabatic state.

in order to account for the presumably Gaussian experimental pump and probe pulse envelopes (both the pump and probe finite laser pulse widths can be taken into account by convoluting the classical trajectory results with a single Gaussian pulse function).[7]

C. NaI Dynamics Results. With all ingredients assembled, we can now examine the photodissociation dynamics of NaI. We consider only those aspects necessary to establish the reasonableness of our potentials/methods in comparison with previous experimental[2,6] and theoretical work[8,9,18] and to provide useful internal comparisons with the NaI·H_2O results to follow.

We first consider the time dependence of the excited adiabatic state population, displayed in Figure 2a, first as determined by the MDQT method and then via a simplified Landau−Zener approach.[32] The former displays an approximate exponential in time decay, with a lifetime of ∼0.2 ps at the initial total energy of ∼4.2 eV. The simple Landau−Zener approach, in which the probability of undergoing a transition to the ground adiabatic state is given by

$$P = \exp\left[-\frac{2\pi\beta^2}{\hbar v|F_{\text{ion}} - F_{\text{cov}}|}\right]$$

where v is the relative velocity in the NaI motion, β is the electronic coupling between the diabatic states, the F's are the forces arising from the diabatic energy curves at the avoided crossing, gives a reasonable, though not highly accurate,

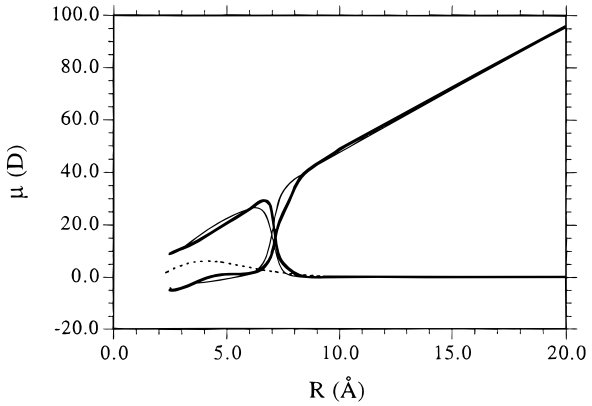

Figure 3. NaI dipole moments. The thick lines are the results of high-level ab initio calculations (MRCI/SD), while the thin lines are the predictions of semiempirical VB theory. Also shown is the transition dipole moment between the semiempirical ionic and covalent VB states (dotted line).

description of the dynamics. It should be noted that the Landau−Zener model[32] assumes that the diabatic curves change linearly in time and that the diabatic basis functions and off-diagonal Hamiltonian coupling matrix elements are independent of time (or diatomic internuclear separation), and thus, the deviation of the MDQT results from the predictions of the Landau−Zener model is indicative of the extent of the shortcomings of these approximations with our NaI potentials.

The calculated probe state signal is displayed in Figure 2b.[33] The probe signal first rises, since the probe state is only accessed in the calculations when the NaI separation corresponds to the outer, ionic portion of the excited adiabatic curve and the overall decline of the excited adiabatic state is evident. In addition, the signal is oscillatory, reflecting the bound motion in the excited adiabatic state. The period is $T = 1.6$ ps at a total energy of 4.2 eV. This is in close agreement both with the results (∼1.7 ps) reported by Zewail and co-workers for the same excitation energy[2a] and with those expected from extrapolation/interpolation of the experimental results of Jouvet et al. (∼1.6 ps).[34]

Accordingly, we consider the present characterization of the NaI system sufficiently realistic to be employed in the more complex NaI·H_2O dimer case, taken up next.

III. NaI·H_2O Characterization

In this section, we describe the charge distribution of NaI and the related interaction potentials with H_2O, as well as the initial ground state distributions and structures for the NaI·H_2O complex.

A. Charge Distributions for NaI States. The dipole moments for the ground and excited adiabatic states of NaI, calculated with semiempirical VB theory—in which the adiabatic states are taken to be linear combinations of semiempirical ionic and covalent VB states—and taken from high-level ab initio calculations,[18] are shown in Figure 3. Also shown is the transition dipole moment between the ionic and covalent VB states predicted by our semiempirical quantum chemistry model. The calculated dipole moments for ground ionic NaI around equilibrium are in very good agreement with the experimental data.[35] For present purposes, the most important feature of the dipole moments in Figure 3 is that the excited adiabatic state polarity is reversed[12,18] in the FC region—where the excited state is predominantly covalent—compared with that of the ground ionic state. This reversal can in fact be qualitatively understood in fairly general terms via simple molecular-orbital arguments[36] for the excited state of a heteronuclear diatomic or a polar bond: the electron density is concentrated on the most electronegative atom in the bonding combination of atomic orbitals, while it is larger on the least electronegative atom for the antibonding combination. Nonetheless, the significant excited state reversed dipole moment, that is, −4.9 D, could be regarded in a sense as initially surprising for alkali halide states, which are usually thought of in terms of simple ionic bonds and nonpolar covalent bonds.[37] In view of the important role that the excited state reversed polarity will subsequently be found to play in the dynamics, we devote some discussion here to its origin in the semiempirical VB perspective used in this work.

In our semiempirical quantum chemistry model, we are correcting for the shortcomings of the valence-only minimum basis set approach—which results in a primitive description of ionic and covalent bonds[37]—not by expanding the basis set but rather by including a mutual polarization energy of the core electrons as a classical polarization potential term in the core−core potential.[16,38] Similarly, the dipole moments of the NaI VB states are computed by summing together the permanent dipole moments arising from the valence-only quantum chemistry charge distribution and the classical induced dipoles that the latter charge distribution induces on the ions/atoms.[38] For the ground state, which is almost purely ionic in the FC region, it works as follows. The ionic VB state point-charge distribution due to the valence electrons is very close to $Na^{+1}I^{-1}$. When adding the permanent dipole moment corresponding to the $Na^{+1}I^{-1}$ species (∼13 D for NaI around equilibrium) to the classical dipole moments induced by the +1 sodium charge on the iodide and by the −1 iodide charge on the sodium ion (minor contribution though, since the polarizability of the sodium ion is fairly small), one obtains a total dipole moment of ∼9.7 D for near-equilibrium ground ionic NaI, which is very close to the experimental value (9.2 D).[35]

For the excited state, which is mainly covalent in the FC region, the simple classical polarization model is comparably successful and allows a proper description of the reversed polarity of the excited NaI state in the FC region. For the latter range of internuclear separations, the covalent VB state point-charge distribution is $Na^{+\delta}I^{-\delta}$ where δ is of the order of ∼0.04. This slight polarization arises from the fact that the valence I 5p Slater orbital is much more diffuse in space than the Na 3s Slater orbital so that there is a net excess electronic density around I. It turns out that these very tiny δ point charges induce significant dipole moments, the sum of which is of the same order of magnitude as that of the ionic state, because of the very large polarizability of the sodium atom (24 $Å^3$)[19] and to a minor extent the polarizability of iodine. Adding the induced dipole moments (which total −4.9 D for NaI in the FC region) to the permanent dipole moment of the covalent state (zero to zeroth-order), we end up with a significant reversed polarity for the covalent NaI state in the FC region.[18] To summarize, in our model, the reversed dipole moment of the "covalent" NaI is due to the polarization of the very polarizable Na atom by a small net excess electron density on the iodine. Overall, the excited adiabatic state is predominantly covalent, and the core classical polarization/semiempirical VB theory thus reproduces the NaI FC state reversed polarity observed in high-level ab initio calculations.[18]

More generally, the dipole moments for both the adiabatic ground and excited states predicted by our classical polarization/semiempirical VB model are in good agreement with high-level ab initio calculations,[18] as shown in Figure 3. Note that if we were using a large atomic basis set, the internal polarization of the VB (or generalized valence bond) states would be properly

described automatically. Thus, the classical polarization model provides a simple correction scheme for the shortcomings of the small basis set framework of semiempirical VB theory.

For describing electrostatic interactions between a solute and water solvent in a simple fashion, one usually resorts to partial point-charge distributions, and the NaI *apparent* point charges associated with the ionic and covalent VB states are extracted from the NaI dipole moments calculated with our classical polarization/semiempirical quantum chemistry approach. For example, the apparent partial charges δ of $Na^{+\delta}I^{-\delta}$ are 0.75 and -0.35 for the ionic and covalent NaI VB states in the FC region, respectively. The latter charge distribution, as we shall see presently, has an important impact on the $NaI{\cdot}H_2O$ photodissociation mechanism and dynamics.

B. Interaction Potentials. The water is described by the rigid TIP4P model,[39] while the NaI−water interactions are described by OPLS potentials,[40] which consist of Coulombic potentials for electrostatic interactions and parametrized Lennard-Jones functions for non-Coulombic dispersion interactions. The parameters for Na^+-H_2O interactions are taken from the early work of Jorgensen and co-workers,[41] while the parameters for I^--H_2O interactions, which have not been reported to our knowledge, were derived in the very same fashion as for other halide−water interactions.[42] The same Lennard-Jones parameters are used for both ion−water and atom−water interactions for simplicity.

Simulations of the photoexcited $NaI{\cdot}H_2O$ dynamics were also performed with a flexible water model,[43] and they showed that energy transfer to water vibrations in the course of trajectories was negligible, indicating that the rigid water model is adequate for the present simulations. Furthermore, the choice of the TIP4P/OPLS potentials, expressed in terms of point charges and dispersion sites, is perfectly compatible with our semiempirical quantum chemistry description of NaI discussed earlier. Also, ab initio calculations[44] indicate that H_2O is slightly more polarized than it is in the gas phase, at least in the ground-state $NaI{\cdot}H_2O$, hence justifying the choice of the TIP4P model for water (the dipole moment of TIP4P water is $\sim$2.2 D, whereas that of gas-phase water is $\sim$1.8 D).[45] The same calculations indicate that the polarity of NaI in both the ground and first excited states is not significantly affected by the presence of a water molecule.

The electronic coupling between the ionic and covalent states is small in the range of diabatic curve crossing ($\leq$2 kcal/mol), which is indicative of the Born−Oppenheimer regime of solvation,[12] where the solvent electrons move much more quickly than the solute electrons so that the solvent effectively "feels" charge-localized solute state charge distributions. As a result, following our earlier work,[12,46] the instantaneous solvation energy for the solute VB state charge distributions is computed and incorporated in the individual Hamiltonian matrix elements, before solving for adiabatic energies.

In our semiempirical VB model, the polarity of NaI in the adiabatic ground and excited states is influenced by the solvent through the *composition* of the adiabatic wave function in terms of the VB states.[12] However, the composition of the latter is not strongly perturbed by the presence of a single water, at least in the FC region of the potentials where the energy gap between the states is much larger than the coupling (the ground state is mainly ionic and the excited state is mainly covalent). Because the presence of a water does not induce a significant change in the polarity of NaI in both the ground and excited states, as observed in the ab initio calculations mentioned above, this suggests that the internal polarization of the ionic and covalent VB states is not strongly affected by the presence of a single water, hence justifying the choice of gas-phase *apparent* point charges for the NaI VB states. At larger NaI internuclear separations, the internal polarization of the VB states is not an issue, since the ionic state consists of separate Na^+ and I^- ions, while the covalent NaI state bears no partial charges.

Finally, the electronic polarizability of the solvent molecule is treated in an average effective way with the TIP4P model potential, and fluctuations in the solvent charge distribution to accommodate instantaneous changes in the solute charge distribution are neglected, in contrast to our earlier solution work,[12] and possible consequences due to this approximation will be investigated later.

C. Ground-State Distributions and Dimer Structures. To account for temperature effects and assess both the stability of the ground ionic $NaI{\cdot}H_2O$ and the cluster distributions at 300 K,[47] Monte Carlo[48] equilibrium simulations were performed.[15] The resulting potential of mean force,[49] which describes the free energy change of the $NaI{\cdot}H_2O$ system as a function of the NaI internuclear separations, and various quantities of interest are shown in Figure 4 as a function of NaI internuclear separation.

From the huge well depth of the potential of mean force, there is no doubt the ground ionic $NaI{\cdot}H_2O$ is stable with respect to dissociation so that photodissociation experiments can be carried out.[31] Further, the average $NaI{\cdot}H_2O$ excitation wavelength and the NaI transition dipole moment die off with increasing NaI internuclear separations, so the absorption intensity for $NaI{\cdot}H_2O$ naturally peaks around the equilibrium ground ionic NaI internuclear separation.

Representative dimer structures are displayed in Figure 5. There it is seen that typically the water molecule is bound to the sodium end of the NaI in the ground ionic state, with a typical Na−O distance of 2.1−2.8 Å and a typical O−I distance of 3.5−4.8 Å. Such a configuration is consistent with the stronger interaction of H_2O with Na^+ (binding energy of $\sim$24 kcal/mol at room temperature)[50] than of H_2O with I^- (binding energy of $\sim$10 kcal/mol at room temperature).[51] The binding energy of an ionic $NaI{\cdot}H_2O$ cluster is $\sim$16 kcal/mol at room temperature, while that of the "covalent" $NaI{\cdot}H_2O$ cluster (structures not shown) is estimated to be only 5 kcal/mol.

Finally, some 20 initial conditions, in both the position and velocity space, for the photoexcited $NaI{\cdot}H_2O$ dynamics were sampled from long runs of Nosé trajectories,[52] thermostated at 300 K, initialized at selected configurations obtained from the Monte Carlo simulations, and performed with a modified version of the velocity Verlet algorithm.[53] Only the subset of the resulting thermal distribution of configurations for which the potential energy gap between the ground and first excited state corresponds to the experimental excitation wavelength (5 eV) is retained.

IV. $NaI{\cdot}H_2O$ Photodissociation Dynamics

In this section, we describe the results and interpretation of the $NaI{\cdot}H_2O$ photodissociation dynamics. The initial conditions are selected as just described, with 5 eV of energy added at time $t = 0$ to the ground state $NaI{\cdot}H_2O$ cluster. The total excess FC energy in the $NaI{\cdot}H_2O$ system is on average 38 ± 2 kcal/mol, with 28 ± 4 kcal/mol in the NaI coordinate and 10 ± 3 kcal/mol nonequilibrium (mainly potential) energy for the NaI−water interactions. Subsequently, various aspects of the dynamics are followed, with the trajectories computed with the MDQT method discussed earlier. For each of the 20 aforementioned classical initial conditions, a swarm of 100 trajectories, that is, a total of 2000 trajectories, are propagated over a 6 ps time scale.

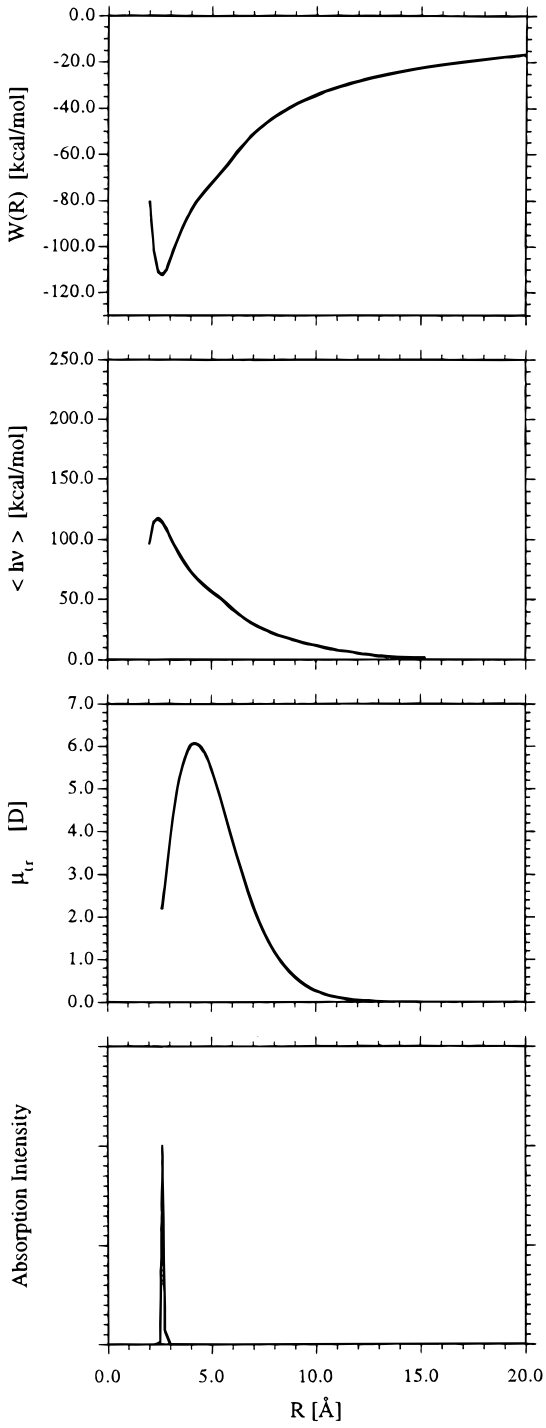

Figure 4. NaI·H_2O equilibrium Monte Carlo simulation results: (a) potential of mean force; (b) average Franck−Condon energy gap (or transition photon energy); (c) transition dipole moment between the semiempirical ionic and covalent NaI VB states; (d) resulting absorption intensity.

A. General Features. We begin with Figure 6a, which displays the excited adiabatic state lifetime dynamics, which is to be compared with the corresponding isolated NaI results in Figure 2a. There is clearly a faster initial loss of excited state population in the NaI·H_2O case, while the longer-time dynamics (>1.5 ps) are quite similar in the two cases.

The first, short time feature is simply related to the stabilization by the H_2O molecule of the outer ionic portion of the excited-state curve, which results in a covalent/ionic crossing point at slightly larger NaI separations (7.5 Å on average) than that in the isolated molecule case (7.1 Å on average). Since

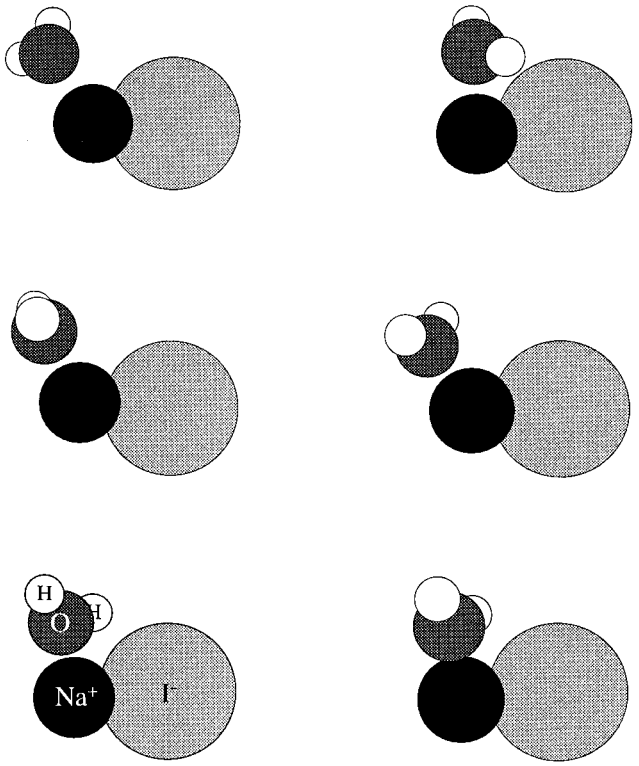

Figure 5. Representative ionic NaI·H_2O complex structures at room temperature.

the crossing probability depends exponentially on the square of the electronic coupling β, and the latter declines exponentially with increasing NaI separation (cf. Figure 1), the probability of remaining on the diabatic covalent curve increases; that is, the probability of an excited to ground adiabatic state transition is enhanced.[54] Further, multiple crossings in the first oscillation period, due to the dynamic stabilization of the ionic state by the nearby water and the resulting time-dependent fluctuation of the relative positions of the diabatic covalent and ionic states, are responsible for enhancing the nonadiabatic transitions to a greater extent. As a result, the excited adiabatic state population in Figure 6a drops sharply—and more rapidly than in the isolated NaI case—at ∼180 fs, when the NaI·H_2O system enters the curve-crossing region for the first time.

The source of the second, longer-time feature is the dissociation or "evaporation" of the water from the complex; this evaporation removes the water from any significant influence in the dynamics, which should then closely resemble those of the isolated NaI. In Figure 7, we display the statistics for this evaporation process. We define the water evaporation time as the time when the smallest of the sodium−water and iodine−water distances exceeds 10 Å, which typically corresponds to interaction energies of a few tenths of a kcal/mol between NaI and water. On average, the H_2O dissociates from the complex in a time scale less than a period of the excited state NaI vibration. This rapid evaporation is suggestive of, and as we will see below, is dominated by, repulsive interactions experienced by the H_2O in the initial FC state.

As a final item in this initial inventory, we note from Figure 6b that the probe signal is still oscillatory in character, though decidedly less so than in the isolated NaI case in Figure 2b.[55] By examination of the individual swarms of trajectories (not shown), this can be traced largely to the fact that the residual energy in the excited state NaI post-H_2O evaporation differs in the various sets of trajectories, resulting in different NaI vibrational frequencies. The distribution of the corresponding

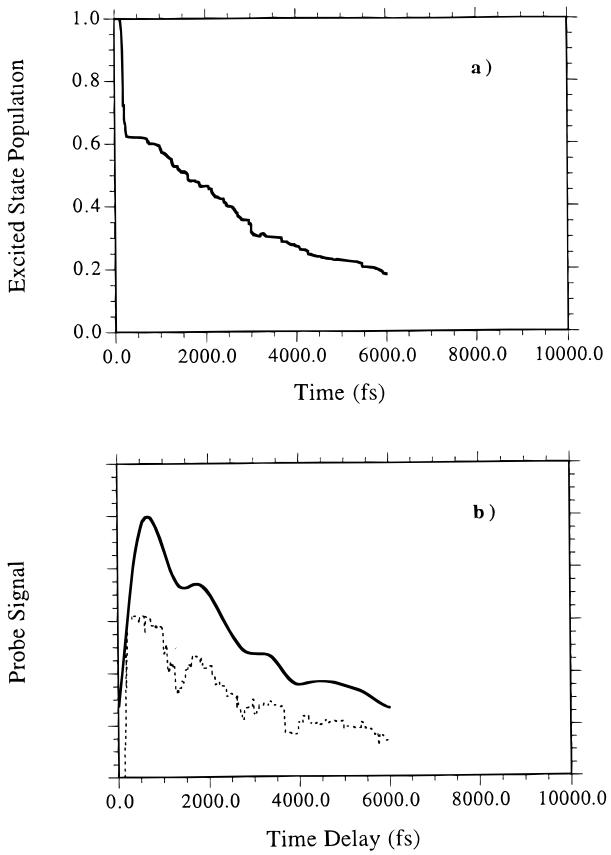

Figure 6. NaI·H_2O photodissociation dynamics results: (a) excited adiabatic state time-dependent population calculated with the MDQT method; (b) Na^+ ion probe signal. The dashed line represents the histogram data collected from the MD simulation, while the solid line represents the simulated signal resulting from a convolution of the histogram results with a Gaussian pulse function.

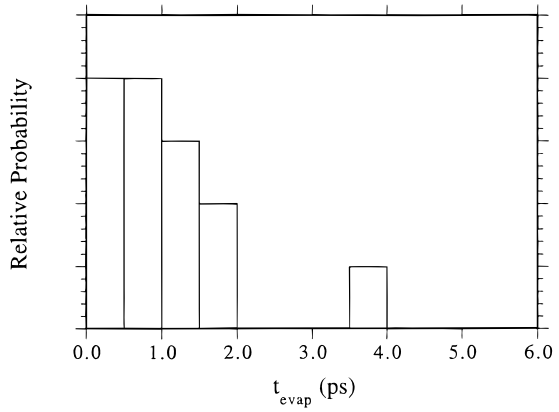

Figure 7. NaI·H_2O photodissociation dynamics: distribution of water evaporation times.

vibrational periods is shown in Figure 8. Nonetheless, oscillatory behavior is still apparent, but with a period (∼1450 fs) that is slightly smaller than for the isolated NaI case (∼1600 fs). But the proper comparison is with the period expected with the initial energy of the excited NaI·H_2O system. In most sampled NaI·H_2O, the initial energy in the NaI coordinate (28 kcal/mol on average) is larger than it is for the isolated NaI (24 kcal/mol) because the FC region corresponding to the 5 eV excitation tends to be shifted toward smaller NaI internuclear separations.[56] So, for instance, adiabatic conservation of the initial FC energy in the NaI vibrational mode would result in an average period of ∼2.3 ps, which is larger than that observed

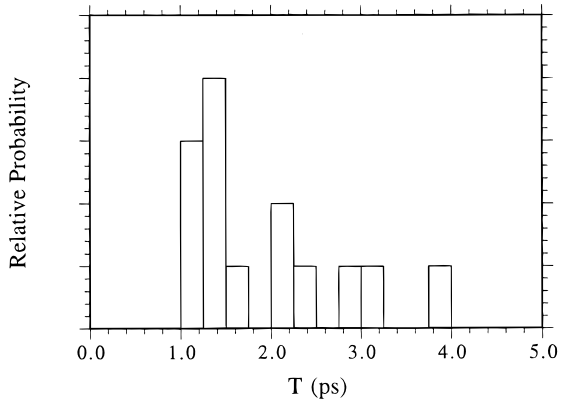

Figure 8. NaI·H_2O photodissociation dynamics: distribution of NaI vibrational periods after H_2O evaporation.

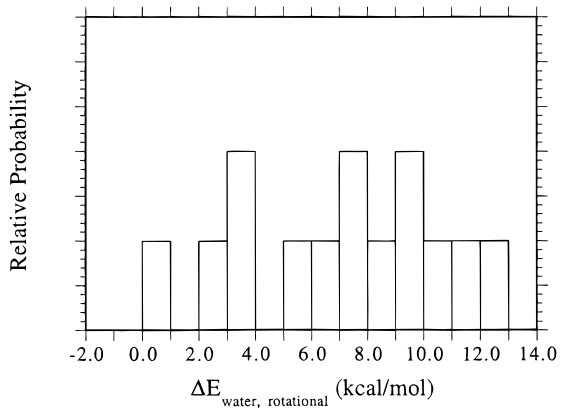

Figure 9. NaI·H_2O photodissociation dynamics: distribution of the final asymptotic rotational energies gained by the water.

in Figure 6b. The reduced period signals that there has been net energy transfer from the excited NaI to the water molecule, leaving the former lower in the excited state adiabatic well, where its frequency is larger. As a matter of fact, an average 20% of the initial FC excess energy in the NaI vibrational coordinate is transferred to the water motion in the photodissociation process.

B. Photodissociation Dynamics. Mechanistic Aspects. Perhaps the most striking features of the photodissociation characteristics recounted above are the indications of rapid "evaporative" dissociation of the water molecule from the cluster involving significant energy transfer out of the NaI system proper. Here, we describe the dominant mechanistic details involved in this phenomenon, as well as the overall process.

We begin with the dominant mechanism observed in the trajectories. In this mechanism, the dominant mode of energy transfer from the excited NaI to the water is into rotational kinetic energy of the latter, as illustrated in Figure 9. Indeed, the water molecule tends to pick up considerable rotational energy in the process. The key to this behavior is the reversed dipole moment in the NaI initially excited FC state, discussed in section III.A. Immediately after the FC transition, the strongest interaction is the repulsion between the Na and I species such that the two begin to separate. Since the iodine is so massive, it is largely stationary and the basic motion is that of the lighter sodium. However, this sodium is partially negatively charged in the initial NaI separation range (cf. Figure 3), which has two consequences. One is that there is a repulsive force on the H_2O oxygen, leading to water translation. The other is that the partially positive water hydrogens are attracted to the leaving $Na^{-\delta}$, and owing to their light mass, considerable

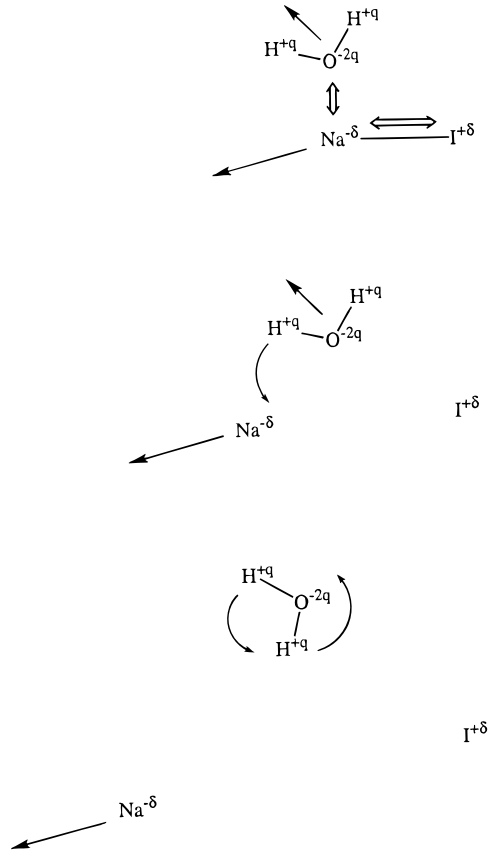

Figure 10. Schematic of the mechanism of water rotational excitation in NaI·H_2O photodissociation dynamics. The double arrows represent repulsions between species, while single arrows describe the relative motion of the species. Attraction of the positively charged water hydrogens to the departing negatively charged sodium causes the water to start rotating, as represented in the middle panel.

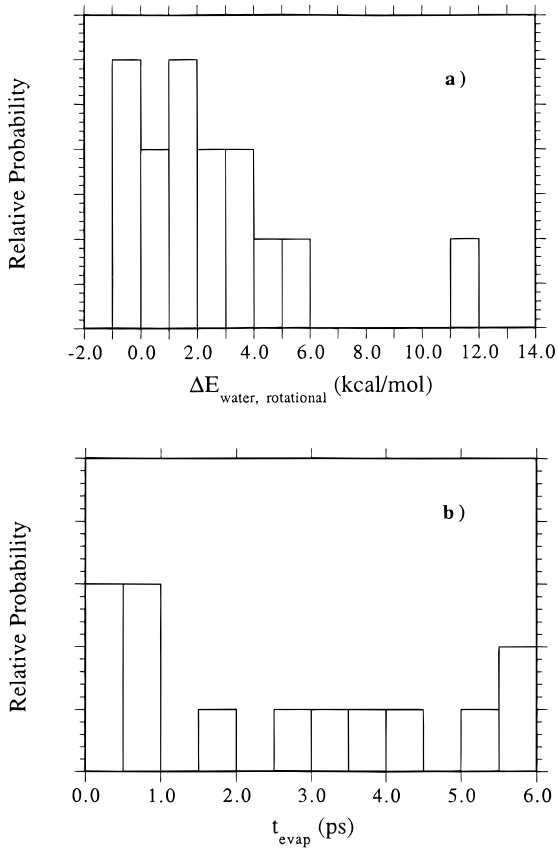

Figure 11. NaI·H_2O photodissociation dynamics with FC NaI state reversed dipole turned off: (a) distribution of the final asymptotic rotational energies gained by the water; (b) distribution of water evaporation times.

rotational excitation of the water results, as schematically shown in Figure 10. As a matter of fact, the average rotational energy gained by water is 6.5 ± 4.5 kcal/mol, while the average translational energy gained by water is only 2.5 ± 3.0 kcal/mol.

The critical role of the FC excited state reversed polarity in the photodissociation/H_2O evaporation process can be directly probed via comparison trajectory calculations in which the excited state reversed polarity is simply turned off; that is, $\mu_{EX} = 0$. Figure 11a, which should be compared with Figure 9, shows that there is much less rotational kinetic energy transferred to the water in the absence of the excited state reversed polarity; the initial electrostatic torque on the H_2O hydrogens is absent. Similarly, Figure 11b, which should be compared with Figure 7, shows that the time for H_2O evaporation on average lengthens considerably without the excited-state reversed polarity; the initial electrostatic repulsive force on the H_2O is absent. As a consequence of the slower water evaporation with the FC excited state reversed polarity turned off, the water keeps interacting with NaI and influences the curve-crossing dynamics beyond the first NaI oscillation period. Thus, if it were not for the FC excited state reversed polarity, the water would be less rotationally hot, would evaporate on a slower time scale, and would influence the curve-crossing dynamics beyond the first NaI oscillation period.

Beyond the above general mechanistic features, we can describe a few further characteristics of the motions, though it should be borne in mind that there can be a wide variation in the details of the various trajectories.

For the majority of the trajectories, the lighter sodium is initially repelled from the nearby stationary iodine, and the water picks up considerable rotational kinetic energy as it starts rotating/spinning in order to accommodate the $O-Na^{-\delta}$ repulsion and the $H-Na^{-\delta}$ attraction, as noted above. In most cases, the water does not pick up enough translational kinetic energy to travel far enough before the NaI becomes more ionic (when internuclear separations of 6−7 Å are reached) and the potential interactions between NaI and H_2O strengthen. The water tends to interact with Na^+ more strongly and effectively as mentioned earlier, but it happens that the water sticks to the I^- in 10% of the trajectories. In both cases, the water stabilizes the outer, ionic branch of the excited state curve. The relative motion of sodium tends to slow down in this region of the excited state well (as less and less kinetic energy becomes available), which allows the water to start equilibrating to Na^+ when it interacts with the latter ion. In cases where the water remains close to I^-, the stationary character of the ion makes it easier for the water to equilibrate to the ion. When the turning point in the excited adiabatic state NaI motion is reached, Na bounces back toward I (after fairly large excursions of 10−25 Å, depending on the energy available for the NaI motion) and the NaI species starts losing its ionic character. The NaI−water interactions become so weak, especially in the NaI internuclear separation range of 5−6 Å, where NaI bears almost no partial charges and the NaI·H_2O binding energy is the smallest, that the water typically evaporates before the end of the first oscillation period (recall that the total NaI·H_2O energy is ∼38 kcal/mol, including initially about 10 kcal/mol in the NaI−water relative motion, and, for example, the binding energy of the "covalent" NaI·H_2O in the FC region is only 5 kcal/mol, while it is much less in the

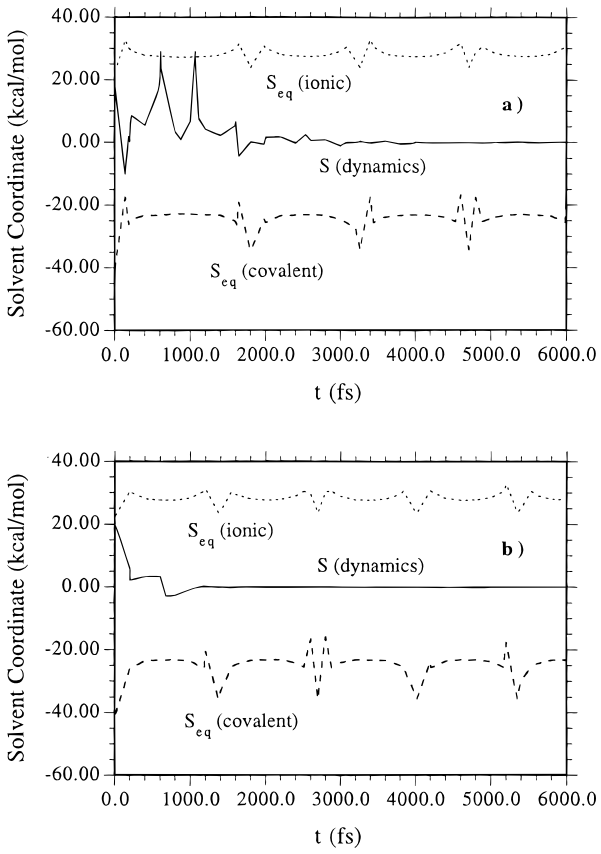

Figure 12. Solvent coordinate in $NaI \cdot H_2O$ photodissociation dynamics. The dashed lines represent equilibrium solvent coordinates and the solid line the actual solvent coordinate along representative trajectories with (a) long-lived $NaI \cdot H_2O$ complex and (b) short-lived $NaI \cdot H_2O$ complex. The solvent coordinate s is defined as the energy gap between the ionic and covalent states solely due to solvation. For a given cluster configuration, $s = V_{ion-sol} - V_{cov-sol}$, where $V_{ion-sol}$ and $V_{cov-sol}$ are the interaction potentials between the solvent water and the ionic and covalent NaI charge distributions, respectively (note that the Lennard-Jones terms, which are the same for the interaction of both states with water, cancel out in the definition of the solvent coordinate, and the latter ends up as the Coulombic energy gap between the states induced by solvation).

NaI internuclear separation range of 5−6 Å). However, in some 15% of the trajectories, the ion−water complex is relatively long-lived (>2 ps), while only in 5% of the cases the complex remains undissociated over the 6 ps trajectory time scale. The relative stability of these long-lived ion−water complexes provides a route for transient formation of $Na^+ \cdot H_2O$ (or $I \cdot H_2O$) on the probe state after probe excitation. Obviously, this is not a frequent occurrence: according to the classical dynamical reflection principle,[8a,b] the calculated signal for $Na^+ \cdot H_2O$ (not shown) versus that of Na^+ is in the ratio 160:1.[57] For completeness, we should also mention another minor class of events (∼15%) observed in the trajectories, in which water initially picks up enough translational kinetic energy to overcome the $NaI \cdot H_2O$ binding energy and departs very quickly (within 400 fs).

Finally, we can emphasize an important point: the extreme nonequilibrium solvation character of the process. The analogue of the solution solvent coordinate can be defined as the solute−solvent interaction energy gap between the diabatic ionic and covalent states.[12] The resulting solvent coordinate along representative trajectories is displayed in Figure 12, together with the hypothetical solvent coordinate for the two diabatic—ionic and covalent—states calculated under the equilibrium solvation condition that the water is equilibrated to that state at each NaI separation $R(t)$ along the trajectory. The periodicity of the equilibrium solvent coordinates is indicative of the periodic motion in the internuclear NaI separation coordinate $R(t)$. In the two cases displayed, one (a) with a long time to H_2O evaporation and the other (b) with a short time, it is clear that H_2O starts out close to equilibrium with the ionic state (trajectory initial condition at 300 K) and that H_2O equilibration is not attained during the time that H_2O interacts with NaI in the excited state. In each case, the very early motion involves an attempt of the H_2O to accommodate to the covalent state, but this is quickly thwarted in case b by H_2O evaporation (resulting in a zero solvent coordinate) and in case a by conversion to the ionic branch of the excited state, where the H_2O attempts to equilibrate to the ionic state, which then converts to the covalent state again, and so forth, before H_2O dissociation. None of this is remotely like the picture painted by the equilibrium solvation curves.

V. Concluding Remarks

In this paper, we have presented a nonadiabatic trajectory study of the photodissociation dynamics of the $NaI(H_2O)$ dimer in the first of a series of papers on the structure and photodissociation dynamics of NaI in cluster systems. We have found that the dynamics are considerably altered from the bare NaI case and, in addition, are characterized by fairly rapid "evaporation" of the water molecule from the cluster. Several of the striking features of the process, including the rotational energy transferred to the water and its rapid evaporation, were shown to be a consequence of the reversed polarity of the excited "covalent" state reached in the initial Franck−Condon transition. An additional feature that we have found in larger water cluster simulations,[15] namely, that the NaI sits on or at the cluster surface, may well lead to other interesting aspects.

Acknowledgment. This research was supported in part by NSF Grants CHE-970049 (University of Colorado) and CHE-9520619 (Colorado State University). J.T.H. thanks Claude Dedonder-Lardeux, Christophe Jouvet, Gilles Grégoire, and other members of the Laboratoire de Photophysique Moléculaire (LPPM) du CNRS (UPR 3361), Université Paris-Sud, Orsay, France for many useful discussions. A portion of this work was performed while J.T.H. was, successively, an Invited Visiting Professor and a CNRS Poste Rouge Research Fellow in the LPPM in Orsay. J.T.H. also gratefully acknowledges receipt of a University of Colorado Research and Creative Work Fellowship (1997−1998) in support of this work. The authors also thank the referees for quite useful comments.

References and Notes

(1) Rosker, M. J.; Rose, T. S.; Zewail, A. H. *Chem. Phys. Lett.* **1988**, *146*, 175. Rose, T. S.; Rosker, M. J.; Zewail, A. H. *J. Chem. Phys.* **1988**, *88*, 6672.

(2) (a) Rose, T. S.; Rosker, M. J.; Zewail, A. H. *J. Chem. Phys.* **1989**, *91*, 7415. (b) Cong, P.; Roberts, G.; Herek, J. L.; Mohktari, A.; Zewail, A. H. *J. Chem. Phys.* **1996**, *100*, 7832.

(3) Cong, P.; Mohktari, A.; Zewail, A. H. *Chem. Phys. Lett.* **1990**, *172*, 109. Mohktari, A.; Cong, P.; Herek, J. L.; Zewail, A. H. *Nature* **1990**, *348*, 225.

(4) Zewail, A. H. *J. Chem. Soc., Faraday Trans.* **1989**, *85*, 1221. Zewail, A. H. *Faraday Trans. Chem. Soc.* **1991**, *91*, 207. Zewail, A. H. *Femtochemistry—Ultrafast Dynamics of the Chemical Bond*; World Scientific: Singapore, 1994. Zewail, A. H. In *Femtosecond Chemistry*; Manz, J., Wöste, L., Eds.; VCH: New York, 1994; Vol. 1, p 15.

(5) Lin, S. H.; Fain, B.; Hamer, N. In *Advances in Chemical Physics*; Prigogine, I., Rice, S. A., Eds.; Wiley: New York, 1990; Vol. 74; p 123.

(6) Jouvet, C.; Martrenchard, S.; Solgadi, D.; Dedonder-Lardeux, C.; Mons, M.; Grégoire, G.; Dimicoli, I.; Piuzzi, F.; Visticot, J. P.; Mestdagh, J. M.; Doliveira, P.; Meynadier, P.; Perdrix, M. *J. Phys. Chem. A* **1997**, *101*, 2555.

(7) Lee, S.-Y.; Pollard, W. T.; Mathies, R. A. *J. Chem. Phys.* **1989**, *90*, 6146.

(8) (a) Engel, V.; Metiu, H. *Chem. Phys. Lett.* **1989**, *155*, 77. (b) Braun, M.; Meier, C.; Engel, V. *J. Chem. Phys.* **1996**, *105*, 530. (c) Engel, V.; Metiu, H.; Almeida, R.; Marcus, R. A.; Zewail, A. H. *Chem. Phys. Lett.* **1988**, *152*, 1. Engel, V.; Metiu, H. *J. Chem. Phys.* **1989**, *90*, 6116.

(9) Martinez, T. J.; Levine, R. D. *Chem. Phys. Lett.* **1996**, *259*, 252. Martinez, T. J.; Levine, R. D. *J. Chem. Phys.* **1996**, *105*, 6334.

(10) Kauzmann, W. *Quantum Chemistry, an Introduction*; Academic: New York, 1957.

(11) Berry, R. S. In *Alkali Halide Vapors*; Davidovits, P., McFadden, D. L., Eds.; Academic: New York, 1979.

(12) Peslherbe, G. H.; Bianco, R.; Hynes, J. T.; Ladanyi, B. M. *J. Chem. Soc., Faraday Trans.* **1997**, *93*, 977.

(13) Grégoire, G.; Mons, M.; Dedonder-Lardeux, C.; Jouvet, C. Is NaI soluble in water clusters? *Eur. Phys. J.*, in press.

(14) See, for example, the following. Amar, F. G.; Berne, B. J. *J. Phys. Chem.* **1984**, *88*, 6720. Perera, L.; Amar, F. G. *J. Chem. Phys.* **1989**, *90*, 7354. Finney, L. M.; Martens, C. C. *J. Phys. Chem.* **1993**, *97*, 13477. Syage, J. A. *J. Phys. Chem.* **1995**, *99*, 5772. Delaney, N.; Faeder, J.; Maslen, P. E.; Parson, R. *J. Phys. Chem. A* **1997**, *101*, 8147. Batista, V. S.; Coker, D. F. *J. Chem. Phys.* **1997**, *106*, 7102.

(15) Peslherbe, G. H.; Ladanyi, B. M.; Hynes, J. T. Structure and Free Energetics of NaI in Water Clusters. A Theoretical Study. Manuscript in preparation.

(16) Peslherbe, G. H.; Ladanyi, B. M.; Hynes, J. T. Nonadiabatic Trajectory Studies of the Photodissociation Dynamics of NaI in Small Water Clusters. Manuscript in preparation.

(17) Mulliken, R. S. *J. Chim. Phys.* **1949**, *46*, 497. Pariser, R. *J. Chem. Phys.* **1953**, *21*, 568. Pohl, H. A.; Rein, R.; Appel, K. *J. Chem. Phys.* **1964**, *41*, 3383.

(18) Sakai, Y.; Miyoshi, E.; Anno, T. *Can. J. Chem.* **1992**, *70*, 309.

(19) *CRC Handbook of Chemistry and Physics*, 77th ed.; Lide, D. R., Ed.; CRC: Boca Raton, Fl., 1996.

(20) For example, ref 6 uses a value of 7 Å^3 for the polarizability of iodine, which seems rather large (e.g., it is larger than the polarizability of iodide).

(21) Tully, J. C. *J. Chem. Phys.* **1990**, *93*, 1061. Tully, J. C. *Int. J. Quantum Chem., Quantum Chem. Symp.* **1991**, *25*, 299. Hammes-Schiffer, S.; Tully, J. C. *J. Chem. Phys.* **1994**, *101*, 4657.

(22) In the original Tully−Preston method [Tully, J. C.; Preston, R. K. *J. Chem. Phys.* **1971**, *55*, 562], the various electronic-states amplitudes in the time-dependent wave function at the diabatic state curve-crossing point determine how trajectories branch out to these states. Alternatively, a Landau−Zener model (see ref 32) was also used to compute transition probabilities or branching ratios.

(23) Alternative methods have been reported to estimate the quantum decoherence time of a system so that quantum amplitudes along a trajectory can be reset at decoherence time intervals, avoiding the need for propagating swarms of trajectories [see, for example, Schwartz, B. J.; Bittner, E. R.; Prezhdo, O. V.; Rossky, P. J. *J. Chem. Phys.* **1996**, *104*, 5942 and references therein]. Although the latter method is particularly economical for condensed-phase simulations, we employ the original trajectory swarm methodology, in the present work, for simplicity.

(24) See, for example, the following. Bala, P.; Grochowski, P.; Lesyng, B.; McCammon, J. A. *J. Phys. Chem.* **1996**, *100*, 2535. Schwartz, B. J.; Bittner, E. R.; Prezhdo, O. V.; Rossky, P. J. *J. Chem. Phys.* **1996**, *104*, 5942. Coker, D. F. In *Computer Simulation in Chemical Physics*; Allen, M. P., Tildesley, D. J., Eds.; Kluwer Academic Publishers: Dordrecht, The Netherlands, 1993; p 315.

(25) Hellmann, J. *Einführung in die Quantenchemie*; Deuticke & Co.: Leipzig, 1937. Feynman, R. P. *Phys. Rev.* **1939**, *56*, 340.

(26) Note that analytic forces, instead of Hellmann−Feynman forces, have also been used in previous nonadiabatic molecular dynamics simulations. See, for example, the following. Maslen, P. E.; Papanikolas, J. M.; Faeder, J.; Parson, R. *J. Chem. Phys.* **1994**, *101*, 5731. Faeder, J.; Delaney, N.; Maslen, P. E.; Parson, R. *Chem. Phys. Lett.* **1997**, *270*, 196.

(27) For a discussion of the Hellmann−Feynman forces in *first-principles* or mixed quantum/classical MD simulations, see for example, the following. Bolton, K.; Hase, W. L.; Peslherbe, G. H. In *Multidimensional Molecular Dynamics Methods*; Thompson, D. L., Ed.; World Scientific: River Edge, NJ, 1997.

(28) Swope, W. C.; Andersen, H. C.; Berens, P. H.; Wilson, K. R. *J. Chem. Phys.* **1982**, *76*, 637. Andersen, H. C. *J. Comput. Phys.* **1982**, *52*, 24.

(29) Verlet, L. *Phys. Rev.* **1967**, *159*, 98.

(30) Press, W. H.; Teukolsky, S. A.; Vetterling, W. T.; Flannery, B. P. *Numerical Recipes, the Art of Scientific Computing*, 2nd ed.; Cambridge University Press: Cambridge, England, 1992.

(31) Jouvet, C.; Dedonder-Lardeux, C. Private communication.

(32) Landau, L. D. *Phys. Z. Sowjetunion* **1932**, *2*, 46. Zener, C. *Proc. R. Soc. London A* **1932**, *137*, 696. Stueckelberg, E. C. G. *Helv. Phys. Acta* **1932**, *5*, 369.

(33) We have also generated the minor signals for the INa^+ species, in reasonable agreement with the results of ref 6. We do not address this species here or subsequently because of its minor role.

(34) The oscillation periods reported in ref 6 are 1260, 1180, and 950 fs for excitation wavelengths of 310, 312, and 347 nm, respectively. A crude interpolation/extrapolation of these results yields a period of ∼1600 fs at 296 nm.

(35) Hebert, A. J.; Lovas, F. J.; Melenders, C. A.; Hollowell, C. D.; Story, T. L.; Street, K. *J. Chem. Phys.* **1968**, *48*, 2834.

(36) See, for example, the following. Atkins, P. W.; Friedman, R. S. *Molecular Quantum Mechanics*; Oxford University Press: New York, 1997; Chapter 8.

(37) In this connection, it is worth pointing out that a primitive semiempirical MO or VB treatment using simple covalent and ionic states (without internal polarization; see the text) gives a small excited state reversed dipole moment of −0.5 D. The latter arises from the cross term $2c_{\mathrm{ion}}c_{\mathrm{cov}}\langle \mathrm{ion}|\mu|\mathrm{cov}\rangle$, where the coefficient of the ionic contribution to the excited state c_{ion} is negative (−0.3). Note that the same primitive treatment predicts a ground state dipole moment of ∼13 D, which roughly corresponds to a (+1, −1) charge distribution for NaI.

(38) The classical electrostatic problem is solved for the dipole moments induced by the point charges on the ion/atom sites [Karplus, M.; Porter, R. N. *Atoms and Molecules; an Introduction for Students of Physical Chemistry*; W. A. Benjamin: New York, 1970; Section 5.3]. The electric field on site i is just the sum of the fields due to the permanent charge and the induced dipole on site j, that is, $\epsilon_i = q_j/(2R^2) + 2\mu_j/R^3$. The induced dipoles, $\mu_i = \alpha_i\epsilon_i$, are solved self-consistently, and the total polarization energy is just $E_{\mathrm{pol}} = \sum\mu_i\epsilon_i$. Note that this is just $-(\alpha_{\mathrm{Na}} + \alpha_{\mathrm{I}})q^2/(2R^4) - 2\alpha_{\mathrm{Na}}\alpha_{\mathrm{I}}q^2/R^7$ for $Na^{+q}I^{-q}$. The ion or atom polarizabilities are smoothly attenuated when decreasing internuclear separations as the effective polarizability of the ions/atoms naturally declines in the presence of other species. Hyperbolic tangents are used as smooth switching functions. For example, the polarizabilities of the sodium and iodine species are reduced by a factor of 0.65 for ionic NaI and 0.75 for covalent NaI at $R = 2.7$ Å in order to reproduce the ab initio dipole moments of NaI.[18]

(39) Jorgensen, W. L.; Chandrasekhar, J.; Madura, J. D.; Impey, R. W.; Klein, M. L. *J. Chem. Phys.* **1983**, *79*, 926.

(40) Jorgensen, W. L.; Severance, D. L. *J. Chem. Phys.* **1993**, *99*, 4233.

(41) Chandrasekhar, J.; Spellmeyer, D. C.; Jorgensen, W. L. *J. Am. Chem. Soc.* **1984**, *106*, 903.

(42) The parameters for the iodide−water OPLS potentials were chosen to reproduce the experimental interaction energy and the calculated HF/3-21+G geometry of the ion−water complex, as was done for fluoride and chloride in ref 41. The resulting Lennard-Jones parameters are $\epsilon = 0.225$ kcal/mol and $\sigma = 3.97$ Å.

(43) Dang, L. X.; Pettitt, B. M. *J. Phys. Chem.* **1987**, *91*, 3349.

(44) Peslherbe, G. H.; Ladanyi, B. M.; Hynes, J. T. Unpublished results.

(45) However, our ab initio calculations seem to indicate that H_2O in the NaI·H_2O first excited state is less polarized than it is in the gas-phase. Thus, our model potentials overestimate the charge−charge interactions between water and NaI in the excited state, which are mainly repulsions in the FC region, due to the reversal of NaI polarity between the ground and excited states. Furthermore, the choice of the same Lennard-Jones parameters for both ionic and covalent VB states leads to an underestimate of, for example, the Na−H_2O binding energy, which reportedly lies in the range 7−11 kcal/mol [Curtiss, L. A.; Kraka, E.; Gauss, J.; Cremer, D. *J. Phys. Chem.* **1987**, *91*, 1080. Ishikawa, Y.; Binning, R. C.; Sekino, H. *Int. J. Quantum Chem., Quantum Chem. Symp.* **1995**, *29*, 669], so the overall stability of the photoexcited NaI·H_2O with respect to dissociation is underestimated and water evaporation is somewhat overestimated in the present calculation.

(46) See also the following. Zichi, D. A.; Ciccotti, G.; Kapral, R.; Hynes, J. T. *J. Phys. Chem.* **1989**, *93*, 6261. Benjamin, I.; Barbara, P. F.; Gertner, B. J.; Hynes, J. T. *J. Phys. Chem.* **1995**, *99*, 7557.

(47) The temperature in NaI cluster experiments is not known precisely and may be lower than this (e.g., 200 K).[31] This is not expected to greatly influence the present results but could be of consequence for larger cluster systems.

(48) Allen, M. P.; Tildesley, D. J. *Computer Simulation of Liquids*; Oxford University Press: New York, 1989.

(49) Hill, T. L. *Statistical Mechanics. Principles and Selected Applications*; McGraw-Hill: New York, 1956.

(50) Dzidic, I.; Kebarle, P. *J. Phys. Chem.* **1970**, *74*, 1466. Kebarle, P. *Annu. Rev. Phys. Chem.* **1977**, *28*, 445.

(51) Hiraoka, K.; Mizuse, S.; Yamabe, S. *J. Phys. Chem.* **1988**, *92*, 3943.

(52) Nosé, S. *Mol. Phys.* **1984**, *52*, 255.

(53) Ciccotti, G.; Ryckaert, J. P. *Comput. Phys. Rep.* **1986**, *4*, 345.

(54) For instance, moving the NaI curve-crossing point from 7.1 to 7.5 Å results in a Landau−Zener nonadiabatic transition probability 7 times larger.

(55) Note that the present detection scheme requires significant access to the ionic portion of the excited state, as discussed in the text. Since this becomes less likely owing to water interaction effects on the excited state (see Figure 6a) and will become increasingly less likely with increasing cluster size (e.g., the discussion in ref 12), other schemes would become preferable. Indeed, a two-photon detection scheme sensitive to the shorter separation covalent portion of the excited state has been developed (Grégoire, G.; Mons, M.; Dimicoli, I.; Piuzzi, F.; Charron, E.; Dedonder-Lardeux, C.; Jouvet, C.; Martrenchard, S.; Solgadi, D.; Suzor-Weiner A. Submitted). In the context of the present calculations, a detection scheme centered on this shorter separation region would only lead to a phase shift in the present results.

(56) The location of the 5 eV FC region for the $NaI \cdot H_2O$ system is mainly governed by the properties of the gas-phase NaI potential curves; the gas-phase energy gap increases towards smaller NaI internuclear separations—from 4.2 eV at the gas-phase FC NaI internuclear separation (the excited state repulsive wall rises more sharply than the ground state potential at small NaI internuclear separations). As a consequence, the 5 eV FC excitation region is shifted toward smaller NaI internuclear separations compared with the gas-phase problem. Meanwhile, the water is reducing this shift toward small NaI internuclear spearations (the water stabilizes the ground ionic NaI state and "destabilizes" the excited state in the FC region; thus, the energy gap between the adiabatic states in the presence of water is larger for a given NaI internuclear separation than it is in the gas-phase). The shift to slightly smaller NaI internuclear separations results in a larger excess energy in the excited state for $NaI \cdot H_2O$ than it is for the isolated NaI (the potential is exponentially repulsive in this region).

(57) In the (very rare) event water evaporates with a lot of, mainly translational, kinetic energy, there is little energy left in the NaI coordinate, that is, less than in the isolated NaI case, and formation of stable INa^+ on the probe state is possible from the excited-state potential outer turning point, where the NaI internal kinetic energy is rather small [see ref 6]. However, if the water leaves with mainly rotational energy (major dissociation pathway), it induces a torque on NaI, with enough associated energy to dissociate INa^+ on the probe state (recall that the probe state is only accessible from the ionic branch of the excited adiabatic state, which corresponds to very small INa^+ binding energies; see Figure 1). As a result, the signal for INa^+ detection determined by the dynamical reflection principle of ref 8a,b is weaker (Na^+/INa^+ signal ratio of 17) than for the isolated NaI photodissociation case (Na^+/INa^+ signal ratio of 6).